PERGAMON

International Journal of Solids and Structures 39 (2002) 4237–4248

INTERNATIONAL JOURNAL OF SOLIDS and STRUCTURES

www.elsevier.com/locate/ijsolstr

Impact failure characteristics in sandwich structures. Part II: Effects of impact speed and interfacial strength

L. Roy Xu [a], Ares J. Rosakis [b,*]

[a] *Department of Civil and Environmental Engineering, Station B 351831, Vanderbilt University, Nashville, TN 37235, USA*
[b] *Graduate Aeronautical Laboratories, California Institute of Technology, Mail Stop 105-50, Pasadena, CA 91125, USA*

Received 25 July 2001; received in revised form 27 February 2002

Abstract

In this paper, we describe the second part of an experimental investigation concentrating on the study of the effects of impact speed and interfacial bond strength on the dynamic failure of model sandwich structures. Results show that even small variations in impact speed and bond strength substantially influence the initiation behavior of delamination (location and nucleation time) and lead to substantially different inter-layer crack speed histories. These changes in inter-layer failure history influence the timing, sequence and final extent of subsequent intra-layer damage within the sandwich structures.

Keywords: Crack arrest; Crack-tip speed; Interfacial strength; Impact speed; Shock wave

1. Introduction

In Part I of this investigation, we have presented and discussed the basic nature and sequence of failure modes in simple layered materials and sandwich structures (Xu and Rosakis, 2002). Results show, that although the dominant failure mechanisms remain unchanged, their sequence and interaction may be strong functions of specimen geometry. Indeed, inter-layer cracking followed by intra-layer cracking remain the two major mechanisms of dynamic failure. One of the major conclusions of Part I of this study is that shear-dominated inter-layer (or interfacial) cracks are the ones that initiate first and that such cracks grow very dynamically, their speeds and shear nature being enhanced by the large wave mismatch between the core and the faceplates. It is the kinking of these cracks into the sandwich core that triggers the complex mechanism of intra-layer failure. It is perhaps intuitively expected that the bond strength between the faceplates and the core as well as the magnitude of the impact pulse will influence the growth characteristics (initiation time and speed) of the interfacial fractures and thus will influence the subsequent failure history.

* Corresponding author. Tel.: +1-626-395-4523; fax: +1-626-449-6359.
E-mail address: rosakis@aero.caltech.edu (A.J. Rosakis).

0020-7683/02/$ - see front matter © 2002 Published by Elsevier Science Ltd.
PII: S0020-7683(02)00246-9

In the past years, dynamic interfacial failure in simple metal/polymer systems has received considerable attention because of its unique characteristics (Lambros and Rosakis, 1995; Liu et al., 1995; Rosakis et al., 1998). Early studies revealed that dynamic interfacial cracks are shear dominated, are often intersonic and they seem to propagate stably and at discreet speeds that are dictated by multiples of the shear wave speed of the slower wave speed constituent of the bimaterial (e.g., Cs). Samudrala and Rosakis (in preparation) and Needleman and Rosakis (1999) also showed that if the interfacial bond strength is changed, the initiation, transition and final choice of stable propagation speeds of interfacial cracks are also dramatically altered. Meanwhile, if the external loading is changed, i.e., the impact speed or pulse duration is altered; significant interfacial crack speed variations were also observed (Samudrala and Rosakis, in preparation). In a recent paper on the impact of laminated and assembled composite plates, Liu et al. (2000) showed that the interface bond strength plays an important role in determining impact resistance.

Based on these preliminary results of the effects of impact speed and interfacial strength on interfacial cracks in simple systems, we try to understand the influence of these important parameters on the impact failure in more complex layered materials and sandwich structures. The major objective of this investigation is to study the effects of different interfacial strengths and impact speeds on inter-layer crack initiation and propagation and on the subsequent transition to intra-layer core damage.

2. Description of experiments

A gas gun impact setup, along with the high-speed photography and photoelasticity arrangements described in Part I of this study, were employed to investigate the dynamic failure phenomenon (Xu and Rosakis, 2002). In order to compare different impact speeds and interfacial strengths, one baseline specimen geometry is chosen, i.e., the short three-layer specimen with equal layer widths (type A specimens in Part I) with two Weldon-10 strong bonds. The baseline impact speed with which the results of this work will be compared to is 33 m/s. This impact situation was extensively discussed in Part I of this study. The specimen, whose length, total width and thickness are 254, 114 and 6 mm respectively, is illustrated in Fig. 1(a). The

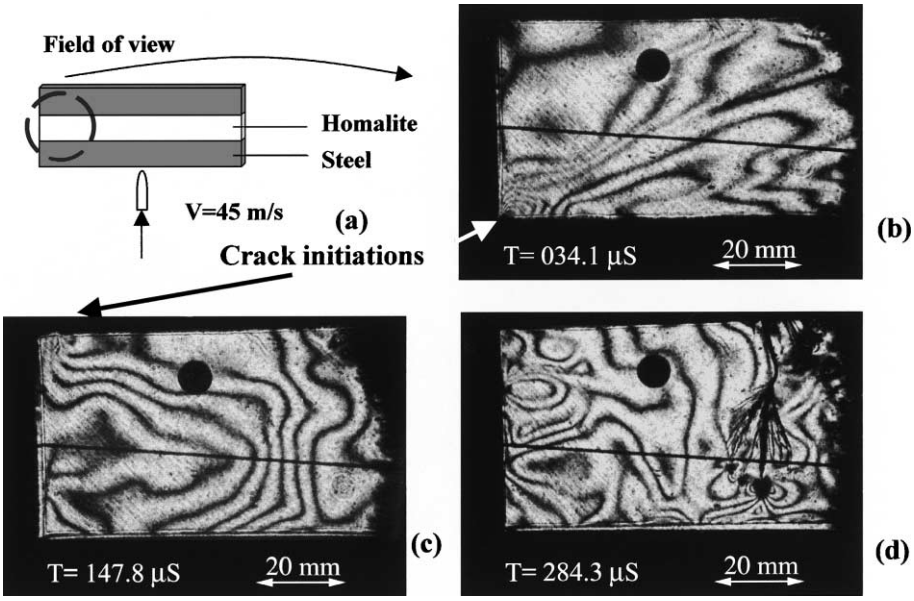

Fig. 1. Failure process at the edge of a specimen featuring two strong interfacial bonds.

material constitution is steel/Homalite/steel and hence dynamic photoelasticity is employed. The details of experimental arrangements were reported in early work by the same authors (Xu and Rosakis, 2002).

3. Results and discussion

3.1. Effect of impact speeds

In Part I of this study, we investigated the nature and sequence of failure mechanisms in relation to model sandwich specimens of the above described geometry and for an impact speed of 33 m/s. This impact speed situation will be taken as the baseline for our comparisons. Fig. 1 describes an experiment of the same geometry that corresponds to an impact speed is 45 m/s. The field of view is the specimen edge.

After impact at the specimen center, the dilatational stress wave propagated towards the edge. Right after the stress wave reached the free edge (due to the existence of stress singularity at the bimaterial corner (Bogy, 1971; Pageau et al., 1996)), an inter-layer crack initiated at the lower interface at around 34 μs as seen in Fig. 1(b). This happened at approximately the same time as in the baseline specimen. This interfacial crack propagated dynamically towards the specimen center. After ≈148 μs, another inter-layer crack initiated at the upper interface as shown in Fig. 1(c). Compared to a crack initiation time of 160 μs for the baseline specimen, this initiation time is slightly shorter but is still within the measurement error range ($0 \sim 10$ μs). This upper inter-layer crack soon interacted with the Rayleigh wave at the lower interface and kinked into the core to form an intra-layer crack. The kinked crack branched into a fan of intra-layer cracks shown in Fig. 1(d). This sequence is very similar to the result of the baseline specimen discussed in Section 3 of Part I.

Despite their apparent similarities, there also exists some noticeable difference between the baseline and the 45 m/s impact cases. The major difference is in the recorded inter-layer, or interfacial crack-tip speeds displayed in Fig. 2(a) and (b). Fig. 2(a) compares the speeds of inter-layer cracks propagating at the lower interface. For an impact speed of 45 m/s, the lower inter-layer crack initially propagated close to the shear wave speed of Homalite-100 becoming clearly intersonic (crack speed less than the longitudinal wave speed but greater than the shear wave speed of Homalite) at ≈60 μs. Throughout its recorded history this crack was clearly faster than its "baseline" counterpart. It should be recalled that at longer time, the baseline crack also became intersonic and reached speeds as high as $\sqrt{2}C_s$ as discussed extensively in Section 3.1 of Part I. Fig. 2(b) compares crack-tip speeds at the upper interfaces. Here again the level of the crack speed

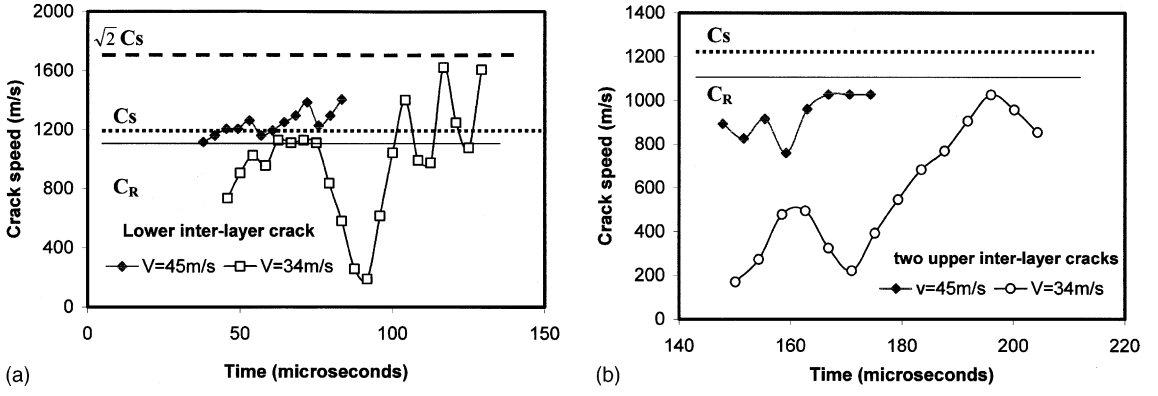

Fig. 2. Comparison of interfacial crack speeds of two identical specimens subjected to different impact speeds. The interfacial bonds are strong Homalite/Weldon-10/steel bonds.

corresponding to 45 m/s impact speed is consistently higher than its baseline counterpart. In both cases, the inter-layer cracks remained purely sub-Rayleigh within our time window of observation.

In order to investigate the crack speed history at the central part of the specimen, the field of view was moved to the specimen center as shown in Fig. 3. The same higher impact speed (45 m/s compared to 33 m/s of the baseline) was employed. As seen from Fig. 3(b), two inter-layer cracks appeared at the lower interface

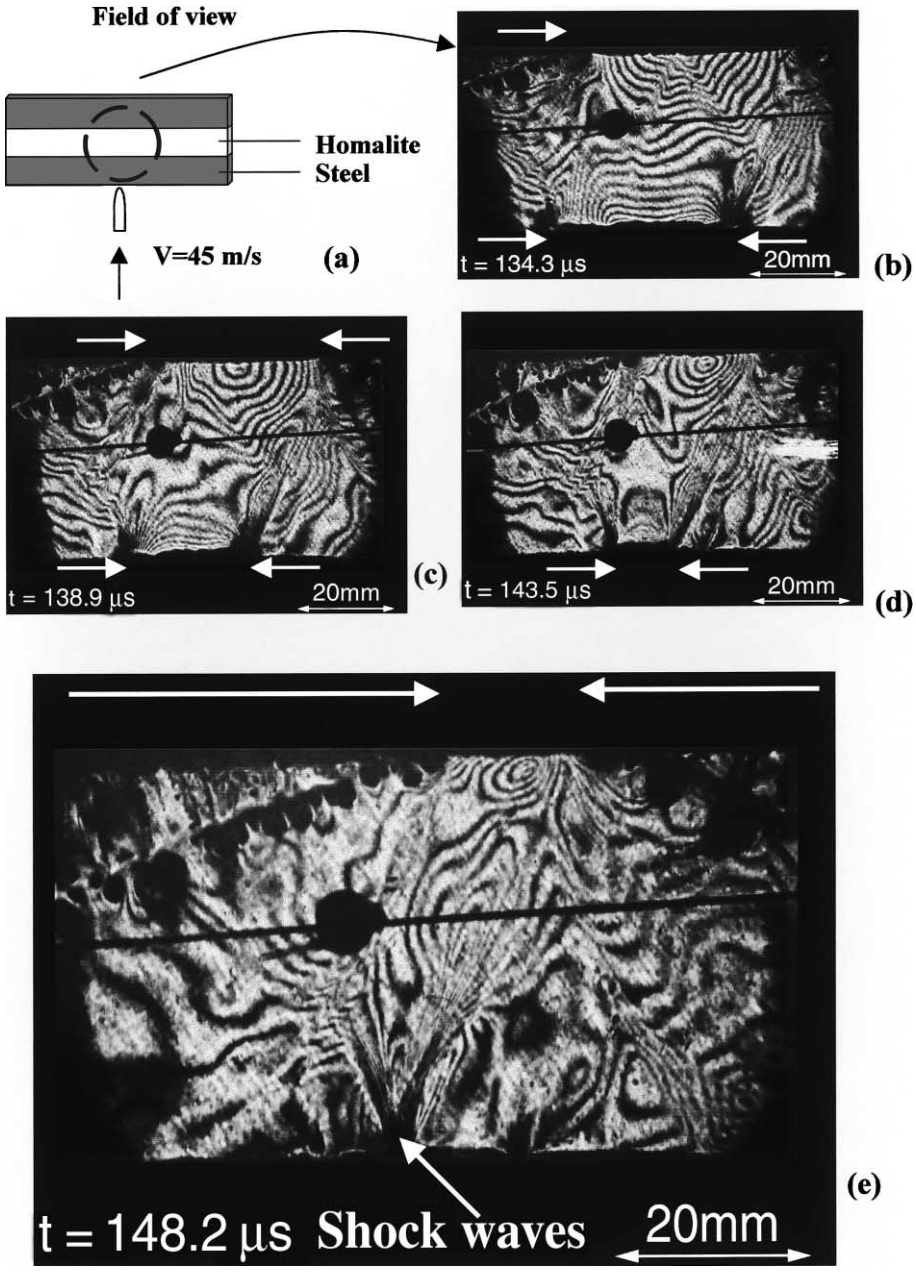

Fig. 3. Growth of four inter-layer cracks at the center of a three-layer specimen (3lshssbwd-6).

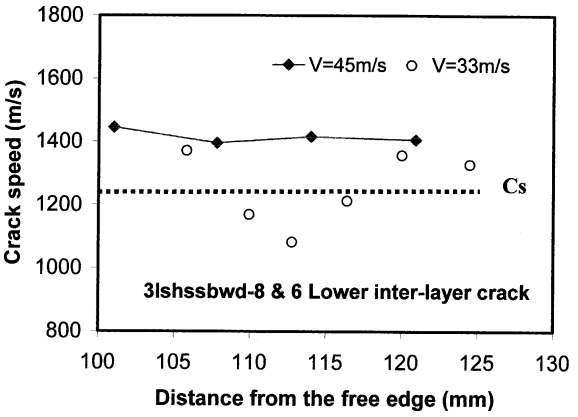

Fig. 4. Comparison of crack speed distributions of two identical specimens subjected to different impact speeds. The dash line is the dynamic shear wave speed Homalite-100.

and propagated towards the center, racing towards each other with intersonic speeds. At a later time, inter-layer cracks at the upper interface also appeared propagating towards the center (Fig. 3(c)). The locations of these four inter-layer cracks (two at the top and two at the lower interfaces) are indicated by the white arrows. As clearly seen from Fig. 3(e), intra-layer damage also spreads from the interface in to the core in the form of a periodic series of mode-I cracks inclined at a small angle to the vertical axis. These cracks are nucleated at the upper interface at locations that are behind the horizontally moving inter-layer shear crack. Their nucleation and growth result in the eventual fragmentation of the specimen core. The inter-layer cracks propagating at the lower bimaterial interface and facing towards each other in Fig. 3(d)–(e) feature clearly formed shock-like or Mach-like discontinuities (shear shock waves) which are emitted from their crack tips. These discontinuities in photoelastic patterns represent traveling discontinuities in maximum shear stress and are clear proofs that crack tips have exceeded the shear wave speed of Homalite (Rosakis et al., 1998). These shock waves formed a clear testimony to the intersonic nature of the inter-layer crack growth even before any detailed crack measurement was ever attempted.

The crack speed history for the lower, right inter-layer crack is plotted in Fig. 4 as a function of distance from the free edge. The figure shows that the crack speed of the higher impact speed case (45 m/s) is always higher than the baseline equivalent remaining always intersonic within the window of observation. To complete the picture, Fig. 5 displays collected experimental results from three identical specimens subjected to the same impact speed, which have areas of observations ranged from the specimen edge all the way to its center. As evident from Fig. 5(a), the inter-layer crack initiated at very high speeds and fluctuated close to the shear wave speed of Homalite, often becoming intersonic but never exceeding $\sqrt{2}C_s$. On the other hand, in the baseline case (33 m/s) and as discussed in Part I, the crack became intersonic only when it approached the specimen centerline. Indeed, before it did so, it almost came to a complete stop at a distance of about 45 mm from the edge.

3.2. Effect of interfacial strengths

In order to compare the effect of different interfacial bond strengths on dynamic failure in layered materials and sandwich structures, four different kinds of adhesives were used to construct interfacial bonds of various strengths. The bond strengths for Homalite/adhesive/Homalite interfaces are listed in Table 1. Due to the stress singularity at bimaterial corners, it is hard to obtain the intrinsic bonding properties of bimaterial interfaces based on current specimen configurations (Xu and Rosakis, in preparation). Instead in

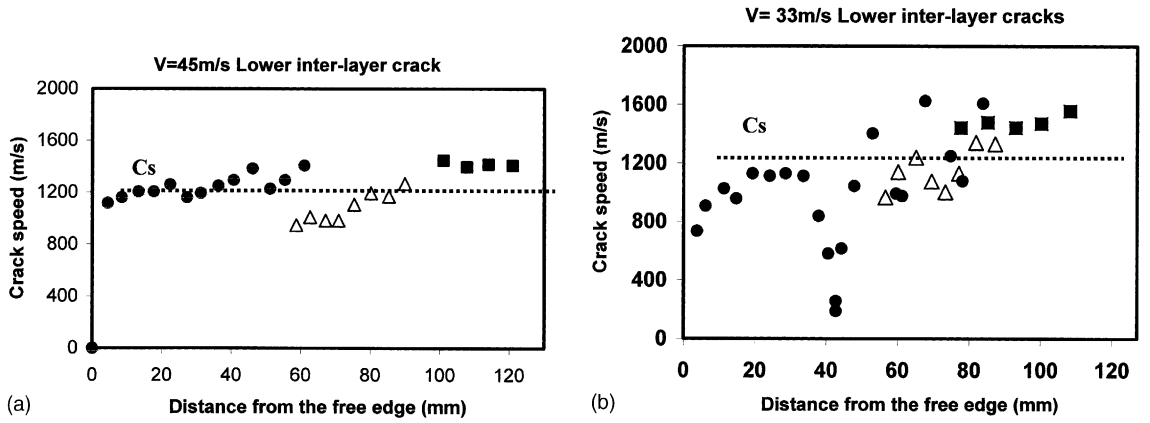

Fig. 5. Comparison of the crack speed distribution along the bond length for identical specimens subjected to different impact speeds.

Table 1
Interfacial strengths and model I fracture toughnesses of different bonds

Interface	Tensile strength (MPa)	Shear strength (MPa)	Fracture toughness (MPa $m^{1/2}$)
Homalite/Weldon-10/Homalite	7.74	>21.65	0.83
Homalite/330/Homalite	6.99	12.58	0.93
Homalite/384/Homalite	6.75	7.47	0.38
Homalite/5083/Homalite	1.53	0.81	0.19

Table 1, we only list the strengths of these adhesives when they are used to bond identical Homalite pieces. This is done to provide relative levels of strengths of these adhesives. The Weldon-10 and Loctite 330 are considered to be "strong" adhesives. The Loctite 384 can form an "intermediate strength" bond while the Loctite 5083 gives a "weak bond". The Loctite 5083 is considered to be a kink of ductile adhesive because its elongation at failure in cured bulk form is as high as 170%. The average thickness of the adhesive layer is less than 20 μm. Here, in order to investigate the relative effect of various interfacial bond strengths, the baseline specimen configuration is chosen as the one shown in Fig. 3, which features the Weldon-10 strong bonding and is subjected to an impact speed of 45 m/s.

Fig. 6 shows a sequence of images of the specimen featuring the second strongest interface, i.e., that of Homalite/330/steel. The field of view is that of the specimen center as shown in Fig. 6(a). The initial failure characteristics in this specimen are quite similar to the ones observed in the baseline specimen with strongly bonded interfaces (i.e., Homalite/Weldon-10/steel), subjected to the same impact conditions as shown in Fig. 3. The first failure mode encountered is still the inter-layer crack at the lower interface. However, for the current case, the two inter-layer cracks separated the entire lower interface at 176 μs after impact as shown in Fig. 6(c) compared to 148 μs in Fig. 3(e). Following inter-layer failure, two intra-layer cracks initiated from the upper interface. Later on and as evident from Fig. 6(d), another mode I intra-layer crack stemmed from the lower interface revealing a locally symmetric fringe pattern and propagating along the specimen centerline. It is speculated that this mode I crack is a result of symmetric specimen bending established at long times after impact. It should be recalled that the shear strength of the 330 bond is much lower than that of the Weldon-10 bond as seen in Table 1. However, the interfacial tensile strength of the 330 bond is only 10% below that of the strong Weldon-10 bond. The differences between these cases discussed here suggest that the interfacial shear strength is vital to the evolution of impact damage in layered materials and sandwich structures.

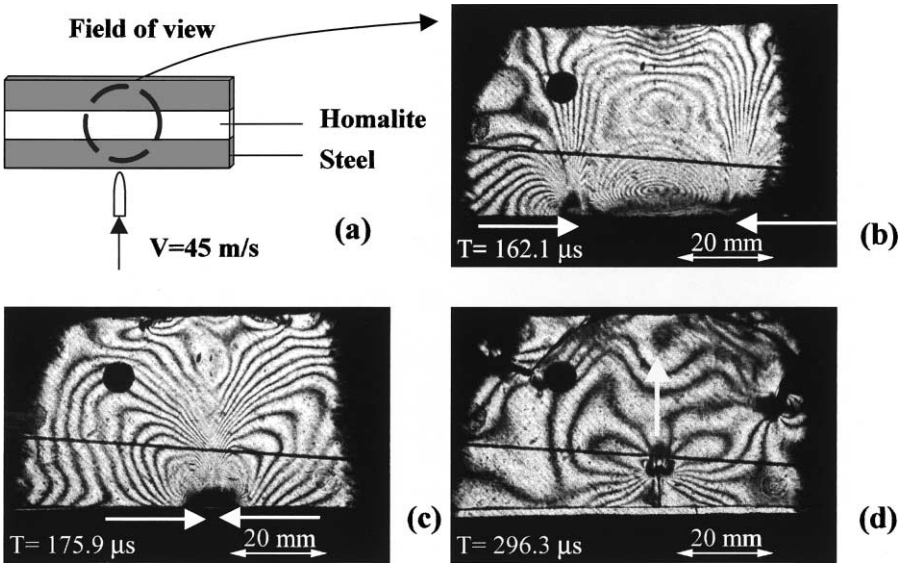

Fig. 6. Different failure modes and sequence in a three-layer specimen with the second strongest bonding (3lshssb330-6). Intra-layer cracks initiated from the upper interface in a symmetric pattern (c) and later on, one intra-layer crack stem from the lower interface (d).

Fig. 7 presents a series of fringe patterns showing the evolution of failure in a specimen featuring intermediate strength 384 adhesive bonds subjected to the same impact condition of 45 m/s. The two lower inter-layer cracks completely debonded the lower interface at 154 μs, slightly later than in the baseline specimen featuring two strong bonds. The upper inter-layer cracks separated the whole upper interface at 207 μs as clearly shown in Fig. 7(e), compared to 157 μs for the specimen featuring the strong Weldon-10 bonds. Similar to the previous case, intra-layer cracks initiated from the upper interface as evident from Fig. 7(f). Although the 384 interfacial bonding is called "intermediate strength bonding," its interfacial tensile strength is only 15% lower than that of the baseline strong bonds. However, its shear strength is substantially lower than that of the strong bonding as listed in Table 1. Here again, it becomes evident that the interfacial shear strength is by itself as an important parameter in controlling the detailed evolution of failure. This is perhaps not very surprising since inter-layer fracture is clearly shear dominated for the layered materials and structures subjected out-of-plane impact loading.

Fig. 8 corresponds to a case where both the interfacial shear and tensile strengths are reduced significantly by using the weak but ductile 5083 adhesive, whose characteristics are also described in Table 1. As shown in Fig. 8(a) and (b), an inter-layer crack generated at the specimen edge is seen propagating towards the impacted point at the specimen center. A thin shear shock line inclined at an angle slightly above 45° to the horizontal interface (Fig. 8(b)) marks the position of this crack which clearly moves intersonically to the right. Since the bond strengths are both very low, the stress concentration appears less strong than in the baseline case (see Fig. 3). Crack-tip speed in this case, however, is very much higher than all other cases and, at the initial stages, is very close to $\sqrt{2}C_s$. To illustrate the strong difference in crack initiation time and in crack-tip speed history between otherwise identical specimens featuring strong and weak bonds, Fig. 9 compares results from the two extreme cases (Weldon-10 and 5083). In both cases, the field of view is concentrated at the specimen edges. It is observed that the weak but ductile 5083 adhesive results in longer initiation time and very high crack-tip speeds. These speeds are initially close to $\sqrt{2}C_s$ then decrease to C_s, and finally pick up as the specimen center is approached. On the hand, the strong Weldon-10 bond features

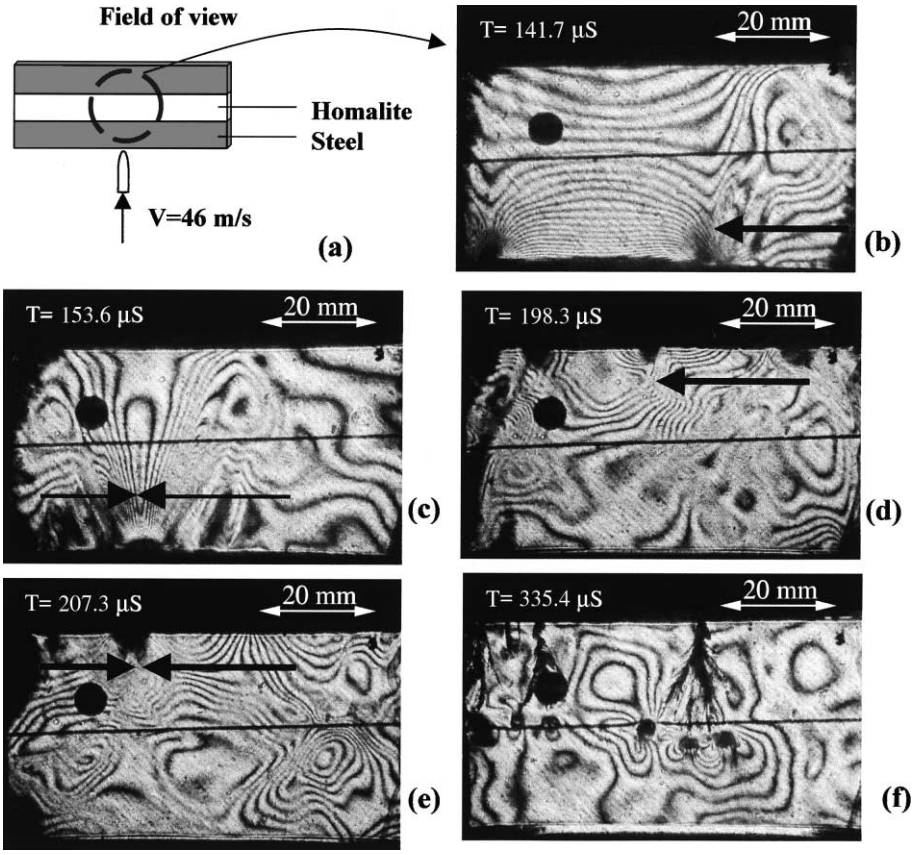

Fig. 7. Failure process of a three-layer specimen with two intermediate strength bonds (3lshssb384-2). After upper interface debonding, two intra-layer cracks initiated from the upper interface and propagated towards the lower interface.

a short initiation time and more moderate speeds ranging from the Rayleigh wave speed to just above the shear wave speed as the distance from the edge increases.

3.3. Dynamic crack arrest and re-initiation

In Part I of this work (Xu and Rosakis, 2002), we observed that the speed of an inter-layer crack decreased to a very low value at around 90 μs after impact (the corresponding position is about 40 mm from the free edge). This phenomenon repeated in other specimens subjected to different loading and bonding conditions. Fig. 10 shows the fringe pattern development of an inter-layer crack at the lower interface of a specimen featuring the second strongest bond in Table 1. A high impact speed of 46 m/s was used, compared to the 34 m/s baseline impact speed in Part I of this paper. After comparing the crack-tip characteristics in Fig. 10(b) and (c), we can see that the fringe concentration delineating the crack tip hardly moved between 98.5 and 117.5 μs. Moreover, the fringe pattern reveals a visibly reduced fringe concentration, which indicates local unloading at the arrested crack tip. The time history of crack lengths and associated crack speeds of two identical specimens subjected to the same impact loading are shown in Fig. 11. The clear plateau of the crack length versus time record reveals the existence of very low crack speeds at a repeatable time and location. It is interesting to notice that crack speed almost drops to zero at around the

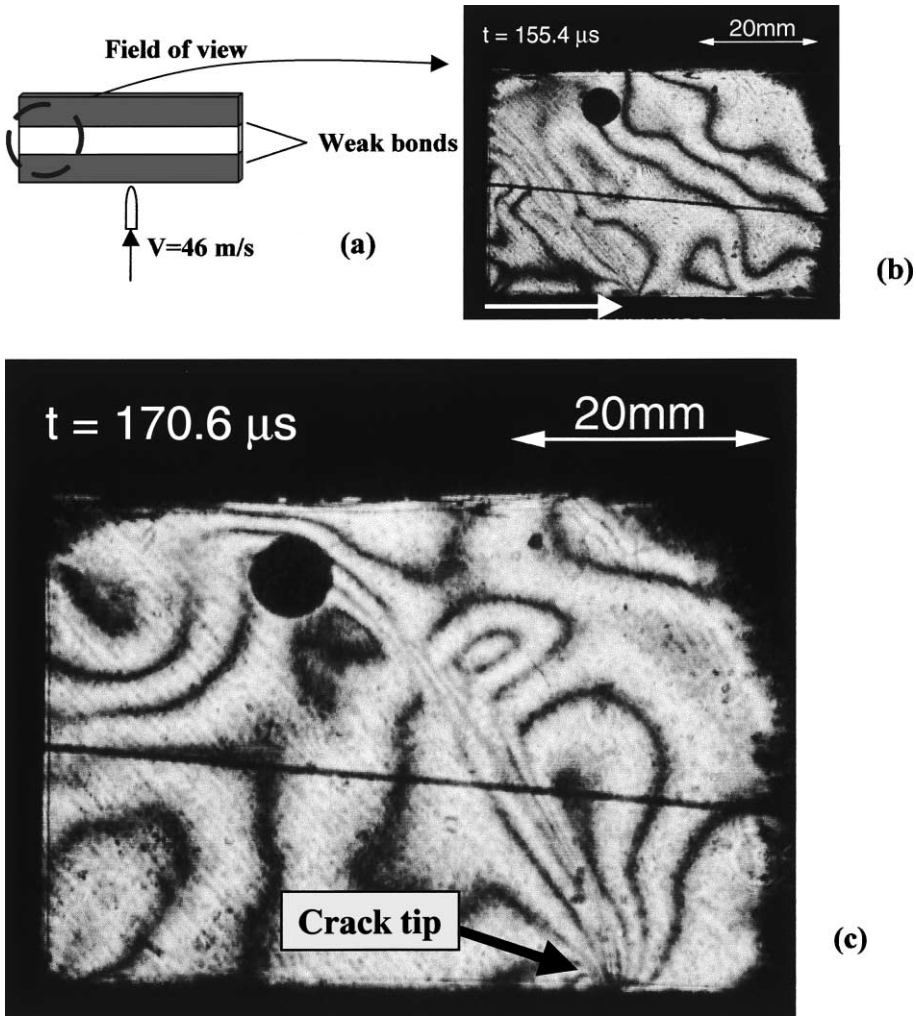

Fig. 8. Intersonic inter-layer crack in a three-layer specimen with weakly bonded interfaces (3lshssb583-1). The crack initiation is delayed but the crack speed is intersonic resulting in a clearly visible shock structure seen in (b) and (c).

same time of 90 μs, as is also reported in Part I of this paper. The location of near crack arrest is also around a distance of 40–50 mm from the specimen edge, exactly as in the strong bond case.

It is theorized here that this phenomenon is associated with the complicated wave interaction and the special characteristics of interfacial cracks at bimaterial interfaces. In previous research on interfacial cracks, Lambros and Rosakis (1995) and Needleman and Rosakis (1999) showed that as soon as an interfacial crack accelerates to the Rayleigh wave speed, it keeps a stable speed as long as constant energy supply is provided to the crack tip. If the energy supply is suddenly increased (perhaps by the arrival of a loading reflected wave from the specimen boundaries), the crack accelerates unstably to another discreet constant level within the intersonic regime. If, however, an unloading wave reaches the crack tip, the crack quickly arrests. We believe that the temporary arrest behavior observed here is a demonstration of the same type of behavior in a more complex structure than the one tested by Lambros and Rosakis (1995) and modeled by Needleman and Rosakis (1999). Here the complex wave interaction and the structural vibration

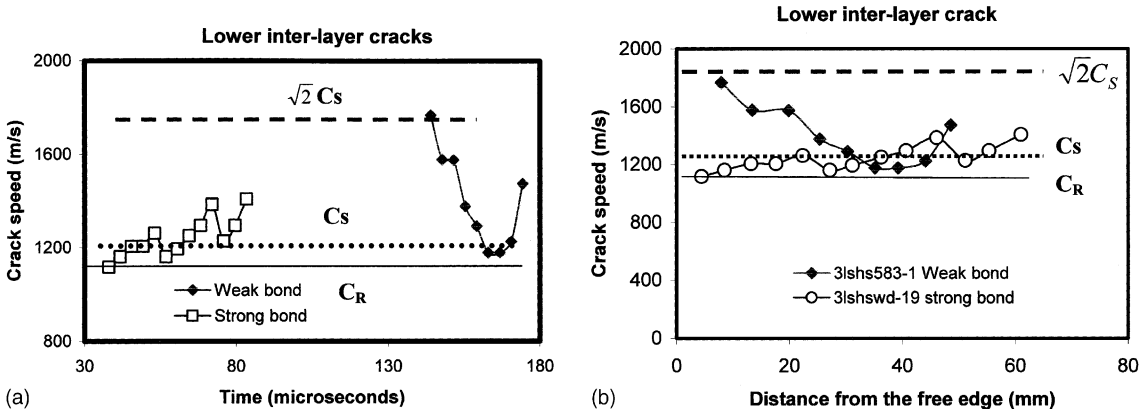

Fig. 9. Crack speed history (a) and crack speed distributions along the specimen length direction (b) for two specimens with different interfacial bond strengths subjected to the same impact loading.

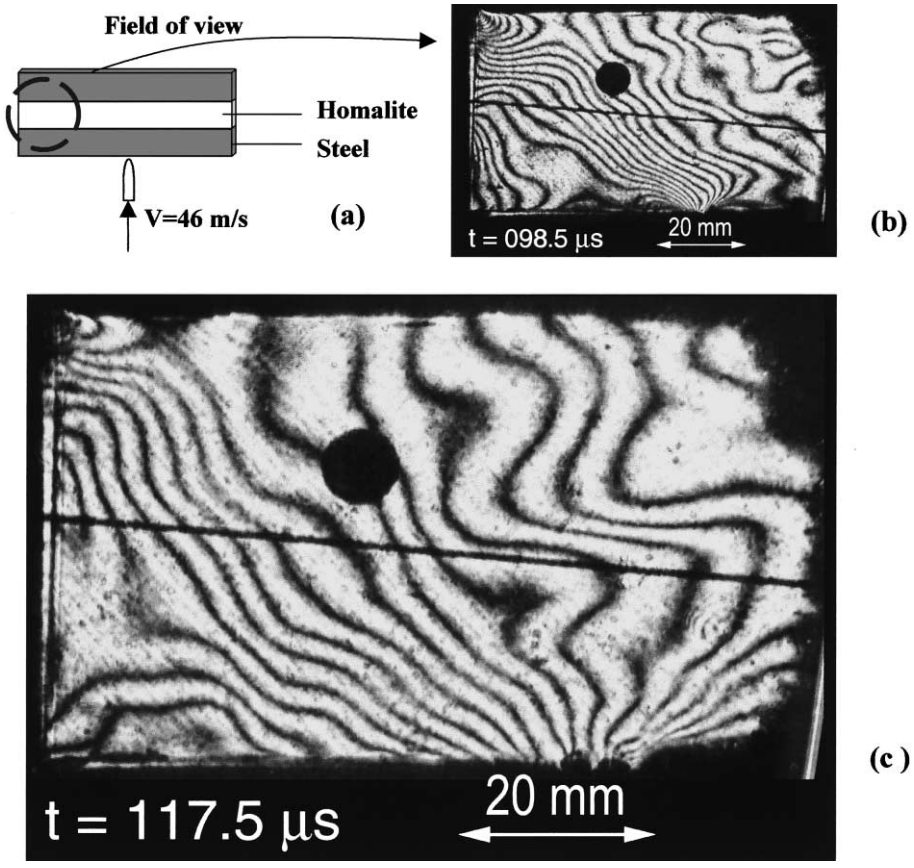

Fig. 10. Visual evidence of the transient inter-layer crack arrest mechanism at the lower interface (3lshssb330-5).

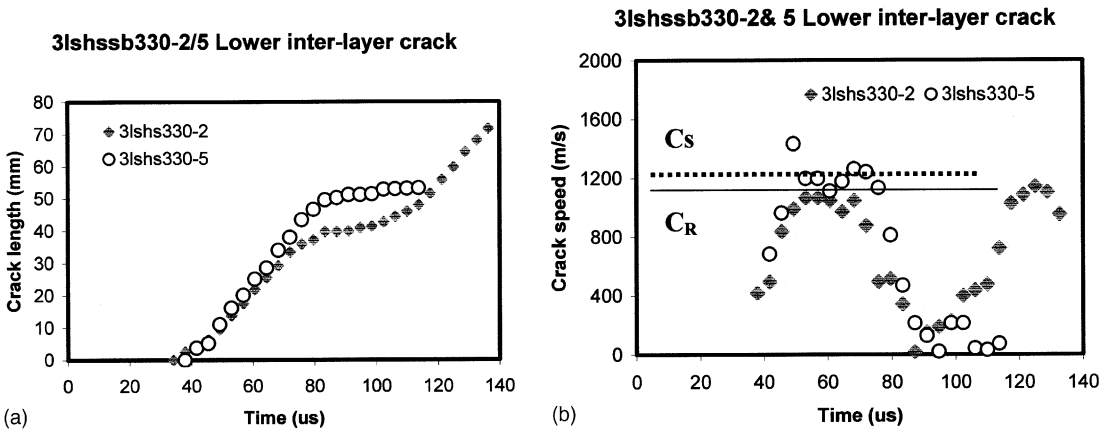

Fig. 11. Time history of crack length (a) and crack speed (b) for two identical specimens featuring the second strongest bonding subjected to the same impact loading.

response of the specimen, which gradually establish themselves with time, result in temporary loss of driving force that accounts for the observed crack arrest and re-initiation. Recently, Yu et al. (2001) successfully simulated this phenomenon.

4. Concluding remarks

High impact loading leads to high inter-layer crack speeds in layered materials and sandwich structures. Strongly bonded specimens subjected to high impact speeds are shown to feature intersonic cracks depending accompanied by the formation of clearly visible shear shock wave (Mach lines) emitted from the crack tips. Reduced interfacial strengths (especially interfacial shear strengths) will result in visible changes of failure sequence. Also, inter-layer cracks at intermediate strength interfaces feature crack speeds slightly slower than those at strong interfaces. However, cracks at weak but ductile interfaces, initiate very late and have a very high speed at the first stage of crack propagation compared to their strong interface counterparts. Finally, highly transient crack arrest and re-initiation phenomenon were observed and analyzed.

Acknowledgements

The authors gratefully acknowledge the support of the Office of Naval Research (Dr. Y.D.S. Rajapakse, Project Monitor) through a grant (#N00014-95-1-0453) to Caltech.

References

Bogy, D.B., 1971. Two edge-bonded elastic wedge of different materials and wedge angles under surface traction. J. Appl. Mech. 38, 377–386.

Lambros, J., Rosakis, A.J., 1995. Shear dominated transonic growth in a bimaterial—I. Experimental observations. J. Mech. Phys. Solids 43, 169–188.

Liu, C., Huang, Y., Rosakis, A.J., 1995. Shear dominated transonic crack growth in a bimaterial—II. Asymptotic fields and favorable velocity regimes. J. Mech. Phys. Solids 43, 189–206.

Liu, D., Basavaraju, B., Dang, X., 2000. Impact perforation resistance of laminated and assembled composite plates. Int. J. Impact Eng. 24 (6–7), 733–746.

Needleman, A., Rosakis, A.J., 1999. The effect of bond strength and loading rate on the conditions governing the attainment of intersonic crack growth along interfaces. J. Mech. Phys. Solids 47, 2411–2449.

Pageau, S.S., Gadi, K.S., Biggers, S.B., Joseph, P.F., 1996. Standardized complex and logarithmic engensolutions for N-material wedges and junctions. Int. J. Fract. 77, 51–76.

Rosakis, A.J., Samudrala, O., Singh, R.P., Shukla, A., 1998. Intersonic crack propagation in bimaterial systems. J. Mech. Phys. Solids 46, 1789–1813.

Samudrala, O., Rosakis, A.J., in preparation.

Xu, L.R., Rosakis, A.J. Comparison of static tensile and shear strengths and fracture toughness of various adhesive bonds between elastic solids, in preparation.

Xu, L.R., Rosakis, A.J., 2002. Impact failure characteristics in sandwich structures; part I: basic failure mode selection. Int. J. Solids Struct., 39(16), 4215–4235.

Yu, C., Ortiz, M., Pandolfi, A., Rosakis, A., 2001. J. Private Communication.